

NLO CORRECTIONS TO HARD PROCESS IN QCD SHOWER — PROOF OF CONCEPT

S. JADACH^a, M. JEŻABEK^a, A. KUSINA^b, W. PŁACZEK^c, M. SKRZYPEK^a

^aInstitute of Nuclear Physics, Polish Academy of Sciences
Radzikowskiego 152, 31-342 Kraków, Poland

^bSouthern Methodist University, Dallas, TX 75275, USA

^cThe Marian Smoluchowski Institute of Physics, Jagiellonian University
Reymonta 4, 30-059 Kraków, Poland

(Received October 16, 2012; revised version received October 30, 2012)

The concept of new methodology of adding QCD NLO corrections in the initial state Monte Carlo parton shower (hard process part) is tested numerically using, as an example, the process of the heavy boson production at hadron–hadron colliders such as LHC. In spite of the use of a simplified model of the process, all presented numerical results prove convincingly that the basic concept of the new methodology works correctly in practice, that is, in the numerical environment of the Monte Carlo parton shower event generator. The differences with the other well established methods, like MC@NLO and POWHEG, are briefly discussed and future refinements of the implementation of the new method are also outlined.

DOI:10.5506/APhysPolB.43.2067

PACS numbers: 12.38.–t, 12.38.Bx, 12.38.Cy

1. Introduction

Successful operation of the Large Hadron Collider (LHC) at CERN is resulting in rich harvest of experimental data. Even more data at higher energy and with higher statistics will be available over the next two decades from the LHC experiments. One of the challenges in the proper understanding and interpretation of these data, possibly leading to discovery of new phenomena, will be perfect mastering of the “trivial” effects due to multiple emission of soft and collinear gluons and quarks. Perturbative Quantum Chromodynamics (pQCD) [1–3], together with the clever modelling of low energy nonperturbative effects, will be the basic and indispensable tool for disentangling the Standard Model physics component in the data.

2. Overview of the method

Most of the methodology used in this work is described in Ref. [4]. In the following, additional details relevant for Monte Carlo (MC) implementation and tests are described. Let us start with a description of the initial condition of the forward evolution (necessary in the MC implementation) which was omitted in Ref. [4]. For the proper understanding of this implementation it is necessary to recall some basic facts about the use of maximum rapidity of emitted partons (angular ordering) as the evolution time variable.

While the energy of the emitted gluon is a natural variable to handle infrared singularities, the angular variable is best suited for controlling collinear singularities. The logarithm of the angle of the emitted gluon (rapidity) with respect to the *emitter parton* emerging from the initial hadron, is a natural “master variable” for modelling collinear singularities. The angular variable is also well suited for modelling the structure of the non-Abelian soft limit (colour coherence) [5–7].

Conversely, a hard process in deep inelastic lepton–hadron scattering (DIS) or Drell–Yan (DY) process acting as a “probe”, either backscattering (in the Breit frame for DIS) or absorbing (into a heavy boson in DY) the emitter parton, in a well defined rest frame of the hard process (RFHP), has its own energy scale used also as a master variable in collinear factorization and renormalization group equations. More precisely, for the hard process with the center-of-mass energy Q (\sqrt{s} in the DY process), the parton entering hard process has the energy equal $Q/2$. On the other hand, in the same RFHP, the initial hadron energy is E_h and the Bjorken variable is the ratio $x = Q/(2E_h)$ (x is invariant with respect to boosts along the emitter direction). The luminosity distribution of this parton $D(Q, x)$ is commonly referred to as parton distribution function, PDF in short. It is weakly dependent on Q and is measured experimentally at each value of Q separately, that is at a given value of Q varying the energy $E_h = Q/(2x)$ of the initial hadron seen in RFHP.

The important practical question for Monte Carlo modelling of the emission of the collinear gluons is: how to relate the variable $\hat{t} = \ln(Q/\Lambda)$ governing the “evolution” of the PDF in the traditional DGLAP schemes¹ such as $\overline{\text{MS}}$ scheme, and the rapidity variable of emitted gluons?

In the following, to answer the above question we shall consider for simplicity the LO case with non-running α_s , and for pure gluonstrahlung (non-singlet QED-like component of PDF) from a *single emitter*². For the MC purpose, we define the evolution variable t as a hypervelocity of the Lorentz

¹ Formulated typically in terms of exponentiation of the collinear singularities or using the renormalization group equations, or both.

² One hemisphere in DY, or initial state cascade/ladder in DIS process.

boost from the initial beam hadron rest frame to RFHP, $t = \Xi$ (or equivalently, the hypervelocity of the beam hadron in the RFHP). For each emitted gluon we define the rapidity ξ_i in the rest frame of the initial hadron, or $\hat{\xi}_i$ in RFHP. Next, we require in the context of pQCD description of the gluonstrahlung that $\hat{\xi}_i < 0$ in the RFHP (in the initial hadron frame $\xi_i < \Xi$). In other words, $t = \Xi$ is a limiting rapidity for emitted gluons (or $\hat{\xi} = 0$). Of course, $e^t = \frac{\sqrt{s}}{m_h} = \frac{Q}{xm_h}$, where m_h is hadron mass and $s = 4E_h^2$.

The role of perturbative QCD is to relate $D(Q, x)$ measured in two experiments A and B with probes at the scales Q_A and Q_B , provided that $Q_A > Q_B \gg m_h$. Two PDFs, $D(Q_A, x)$ and $D(Q_B, x)$, will differ because of the gluon emissions located in the additional phase space within the (Ξ_A, Ξ_B) rapidity (angular) interval. Also, experiments A and B will use different RFHPs, connected by the Lorentz boost of the hypervelocity $\Delta t = \Xi_A - \Xi_B = \ln \frac{Q_A x_B}{Q_B x_A}$.

What is now the difference between the more traditional choice of the evolution time variable $\hat{t} = \ln \frac{Q}{\Lambda}$ of DGLAP and our preferred definition $t = \Xi = \ln \frac{E_h}{m_h} \Big|_{\text{RFHP}} = \ln \frac{Q}{xm_h}$ (maximum rapidity of the emitted gluons)? When comparing two experiments with hard probes at the scales Q_A and Q_B , $\Delta \hat{t} = \ln(Q_A/Q_B)$, while more phase-space conscious $\Delta t = \Delta \hat{t} - \ln(x_A/x_B)$. The “offset” $\ln(x_A/x_B)$ is formally of the NLO class³ and can be neglected within the LO approximation⁴, hence both choices are equally good at LO level. However, the use of (angular) t assures the completeness of the phase space of the emitted gluon, no gaps (nor “dead zones”), so it is the preferred choice in the MC modelling, aiming at the NLO level evolution in the next steps. Additionally, the parallel use of $\hat{t} = t - \ln \frac{\Lambda}{xm_h}$ is quite useful and essential for other purposes, like introduction of the running α_s , *etc.*

In particular, \hat{t} is more natural for defining the initial point of the forward evolution (the stopping rule in the backward evolution). In order to assure the validity of pQCD, it is required that the energy scale of the probe $q_0 \gg \Lambda, m_h$ is reasonably above the non-perturbative scales, like $\Lambda \simeq m_h \simeq 1 \text{ GeV}$, at the above initial point. This leads to the initial forward evolution point at $\hat{t}_0 \simeq \ln(q_0/\Lambda)$ and $t_0 \simeq \ln(q_0/m_h) - \ln x_0$, as implemented in the following MC. In other words, gluons with rapidities below t_0 are regarded as “unresolved”, *i.e.* $t_0 = \xi_0$ is a maximum rapidity for all unresolved gluons.

It should be noted that the above discussion is quite standard in the context of any Monte Carlo parton shower using the angular ordering. This line of the MC parton shower inspired by the CCFM model [8, 9], see

³ It induces extra $\mathcal{O}(\alpha_s)$ term in the evolution kernel.

⁴ We have to remember to take it into account at the NLO level, when defining NLO evolution kernel.

also Refs. [9–11], is presently developed by the authors of the CASCADE MC [12]. In particular, when using (maximum) rapidity t as the evolution time variable in the time ordered exponential of the QCD parton distributions the complete multigluon phase space is covered (with no gaps, “dead zones”), while the straightforward use of the ordering in the \hat{t} variable in the MC would result in gaps between emitted real hard gluons, see also brief discussion of the corresponding kinematics in Ref. [13].

2.1. Single LO ladder — basic building block in the MC

Let us define multigluon distribution in the single initial state ladder taken in the LO approximation, which is a building block in our parton shower MC implementation, as an integrand in the following “exclusive/unintegrated PDF”

$$\begin{aligned}
 D(t, x) &= \int dx_0 dZ \delta_{x=x_0 Z} d_0(\hat{t}_0, x_0) G(t, \hat{t}_0 - \ln x_0 | Z), \\
 G(t, t_0 | Z) &= e^{-S_F} \sum_{n=0}^{\infty} \left(\prod_{i=1}^n \int d^3 \mathcal{E}(\bar{k}_i) \theta_{\xi_i > \xi_{i-1}} \frac{2C_F \alpha_s}{\pi^2} \bar{P}(z_i) \right) \\
 &\quad \times \theta_{t > \xi_n} \delta_{z=\prod_{j=1}^n z_j}, \tag{1}
 \end{aligned}$$

where $\bar{P}(z) = \frac{1}{2}(1+z^2)$, $\hat{t}_0 = \ln(q_0/\Lambda)$. The “eikonal” phase space integration element is defined as in Ref. [4]⁵

$$d^3 \mathcal{E}(k) = \frac{d^3 k}{2k^0} \frac{1}{\mathbf{k}^2} = \pi \frac{d\phi}{2\pi} \frac{dk^+}{k^+} d\xi$$

and $k^\pm = k^0 \pm k^3$. In the above, we use rapidity $\xi = \frac{1}{2} \ln \frac{k^-}{k^+} \Big|_{\text{Rh}}$ defined in the beam hadron rest frame Rh, while $\eta = \frac{1}{2} \ln \frac{k^+}{k^-} \Big|_{\text{RFHP}}$ of Ref. [4] was defined in laboratory frame⁶. They are simply related by $\xi = \ln \frac{\sqrt{s}}{m_h} - \eta$. Rapidity ordering is now $t = \xi_{\max} > \xi_n > \dots > \xi_i > \xi_{i-1} > \dots > \xi_0 = t_0$, where $t_0 = \xi_0 = \ln(q_0/m_h) - \ln x_0$. The direction of the z axis in the RFHP is traditionally pointing out towards the hadron momentum. A lightcone variable of the emitted gluon is defined in the usual way as $\alpha_i = \frac{2k_i^+}{\sqrt{s}}$, of the emitter (after i emissions) as $x_i = x_0 - \sum_{j=0}^i \alpha_j$, and finally $z_i = x_i/x_{i-1}$.

⁵ A single ladder (parton shower from single emitter) is defined in the “tanget space” of momenta \bar{k} , see Ref. [4].

⁶ Or, alternatively, in the overall center of the mass system.

The Sudakov formfactor S_F is determined by the “unitarity” condition

$$\int_0^1 dZ G(t, t_0|Z) = 1 \quad (2)$$

and we omit its explicit definition, which involves the usual cut-off $1 - z_i < \epsilon$ regularizing the IR singularity $\frac{d\alpha_i}{\alpha_i} = \frac{dz_i}{1-z_i}$. The above feature is instrumental in the Markovian MC implementation, which provides $D(t, x)$ for any value of $t > t_0$.

The initial distribution $d_0(q_0, x_0)$ can be related to experiment, to previous steps in the MC ladder, or to PDF in the standard $\overline{\text{MS}}$ system. Its precise definition is not essential for the following tests of implementation of the NLO corrections to the hard process, hence we will define it only numerically. We only notice that due to Eq. (2) the baryon number conservation sum rule

$$\int_0^1 dx D(t, x) = \int_0^1 dx_0 d_0(t_0, x_0)$$

is preserved.

Finally, note the use in Eq. (1) of the rescaled four-momenta \bar{k}^μ within the “tangent space”, as defined in Ref. [4]. The mapping $k^\mu \rightarrow \bar{k}^\mu$ can be defined⁷ once the ladders are connected together with the hard process, back in the common standard Lorentz invariant phase space, see Ref. [4] and the following sections.

2.2. Two-ladder LO multiparton distributions

As a necessary introductory step to correcting the hard process to NLO level, let us start with defining and testing our simplified MC parton shower implementing the DY process with two ladders and the hard process, all three in the LO approximation⁸

⁷ This mapping preserves the rapidity variable.

⁸ In this work, we adopted notation of Ref. [4], in particular $d\tau_2(P; q_1, q_2) = \delta^{(4)}(P - q_1 - q_2) \frac{d^3 q_1}{2q_1^0} \frac{d^3 q_2}{2q_2^0}$.

$$\begin{aligned}
\sigma_0 = & \int dx_{0F} dx_{0B} d_0(\hat{t}_0, x_{0F}) d_0(\hat{t}_0, x_{0B}) \sum_{n_1=0}^{\infty} \sum_{n_2=0}^{\infty} \int dx_F dx_B \\
& \times e^{-S_F} \int_{\Xi < \eta_{n_1}} \left(\prod_{i=1}^{n_1} d^3 \mathcal{E}(\bar{k}_i) \theta_{\eta_i < \eta_{i-1}} \frac{2C_F \alpha_s}{\pi^2} \bar{P}(z_{Fi}) \right) \delta_{x_F=x_{0F}} \prod_{i=1}^{n_1} z_{Fi} \\
& \times e^{-S_B} \int_{\Xi > \eta_{n_2}} \left(\prod_{j=1}^{n_2} d^3 \mathcal{E}(\bar{k}_j) \theta_{\eta_j > \eta_{j-1}} \frac{2C_F \alpha_s}{\pi^2} \bar{P}(z_{Bj}) \right) \delta_{x_B=x_{0B}} \prod_{j=1}^{n_2} z_{Bj} \\
& \times d\tau_2 \left(P - \sum_{j=1}^{n_1+n_2} k_j; q_1, q_2 \right) \frac{d\sigma_B}{d\Omega}(sx_F x_B, \hat{\theta}) W_{MC}^{NLO}. \quad (3)
\end{aligned}$$

In the LO approximation, we set $W_{MC}^{NLO} = 1$. This weight will be defined/restored in the next section. In the above, we use rapidity variable η , defined in the overall center of the mass system (CMS). Rapidity ξ of Eq. (1) is translated into η , differently in the forward part (F) of the phase space $\eta_{0F} > \eta_i > \Xi$, where we define $\xi_i = \ln \frac{\sqrt{s}}{m_h} - \eta_i$, and in the backward (B) part $\Xi > \eta_i > \eta_{0B}$, where $\xi_i = -\ln \frac{\sqrt{s}}{m_h} + \eta_i$ should be used. The boundary between the two hemispheres Ξ is for the moment set to be at $\Xi = 0$, but in a more sophisticated versions of the MC will be correlated with the position of the produced heavy boson (LO), or heavy boson and the hardest gluon (LO+NLO)⁹. For the initial condition in the evolution we define $\eta_{0F} = \ln(q_0/m_h) - \ln(x_{0F})$ and $\eta_{0B} = -\ln(q_0/m_h) + \ln(x_{0B})$. However, for the sake of simplicity we will set $\ln(q_0/m_h) = 0$ in the following.

Phase space integration of Eq. (3) for $W_{MC}^{NLO} = 1$ and using Eq. (1), provides us with the classical factorization formula

$$\sigma_0 = \int_0^1 dx_F dx_B D_F(t, x_F) D_B(t, x_B) \sigma_B(sx_F x_B). \quad (4)$$

In testing numerically the above formula, the convolutions $D_F(t, x_F) = (d_0 \otimes G_F)(t, x_F)$ and $D_B(t, x_B) = (d_0 \otimes G_B)(t, x_B)$ are obtained from separate simple Markovian LO Monte Carlo exercises. As was stressed in Ref. [4], the above LO formula represents our LO MC without any approximations and can be tested with arbitrary numerical precision. Such a precise numerical test is demonstrated in the next section.

⁹ Gluon phase space is always fully covered (no gaps).

In Eq. (3) distributions are expressed (similarly as in Eq. (1)) in terms of the \bar{k}^μ four-momenta in the tangent space. The mapping $\bar{k}^\mu \rightarrow k^\mu$ is understood to be exactly the same as defined in Ref. [4], that is done simultaneously for both hemispheres, using ordering in the variable $|\eta_i - \Xi|$. The details of this mapping do not influence the validity of Eq. (4).

2.3. Two LO ladders and NLO-corrected DY hard process

Introduction of the NLO corrections to the hard process is done using a single “monolithic” weight $W_{\text{MC}}^{\text{NLO}}$ on top of the LO distributions of Eq. (3). In the following numerical exercises we will implement $W_{\text{MC}}^{\text{NLO}}$ defined exactly as in Ref. [4]. Let us recall this definition in a slightly more compact notation, for the sake of completeness

$$W_{\text{MC}}^{\text{NLO}} = 1 + \Delta_{\text{S+V}} + \sum_{j \in \text{F}} \frac{\tilde{\beta}_1(q_1, q_2, \bar{k}_j)}{\bar{P}(z_{\text{F}j}) d\sigma_{\text{B}}(\hat{s}, \hat{\theta})/d\Omega} + \sum_{j \in \text{B}} \frac{\tilde{\beta}_1(q_1, q_2, \bar{k}_j)}{\bar{P}(z_{\text{B}j}) d\sigma_{\text{B}}(\hat{s}, \hat{\theta})/d\Omega}, \quad (5)$$

with the NLO soft+virtual correction $\Delta_{\text{V+S}} = \frac{C_{\text{F}}\alpha_{\text{s}}}{\pi} \left(\frac{2}{3}\pi^2 - \frac{5}{4} \right)$ and the real correction part

$$\begin{aligned} \tilde{\beta}_1(q_1, q_2, k) = & \left[\frac{(1-\beta)^2}{2} \frac{d\sigma_{\text{B}}}{d\Omega_q}(\hat{s}, \theta_{\text{F}}) + \frac{(1-\alpha)^2}{2} \frac{d\sigma_{\text{B}}}{d\Omega_q}(\hat{s}, \theta_{\text{B}}) \right] \\ & - \theta_{\alpha > \beta} \frac{1 + (1-\alpha-\beta)^2}{2} \frac{d\sigma_{\text{B}}}{d\Omega_q}(\hat{s}, \hat{\theta}) \\ & - \theta_{\alpha < \beta} \frac{1 + (1-\alpha-\beta)^2}{2} \frac{d\sigma_{\text{B}}}{d\Omega_q}(\hat{s}, \hat{\theta}). \end{aligned} \quad (6)$$

The above represents the exact ME of the quark–antiquark annihilation into a heavy vector boson process with additional single real gluon emission¹⁰ and subtraction of the LO component already included in the LO MC. The angle θ in the subtraction (LO) part of the Born distribution is typically defined in the rest frame of the heavy boson, where $\vec{q}_1 + \vec{q}_2 = 0$, as the angle between the decay lepton momentum \vec{q}_1 and the difference of momenta of the incoming quark and antiquark $\hat{\theta} = \angle(\vec{q}_1, \vec{p}_{0\text{F}} - \vec{p}_{0\text{B}})$ ¹¹, while two angles in the NLO exact ME are defined precisely as $\hat{\theta}_{\text{F}} = \angle(\vec{q}_1, -\vec{p}_{0\text{B}})$ and $\hat{\theta}_{\text{B}} = \angle(\vec{q}_1, \vec{p}_{0\text{F}})$. (The implementation of NLO corrections in POWHEG scheme in Ref. [15] uses the same form of the exact ME.) Note that in the

¹⁰ We employ here the particular compact representation of Ref. [14] of this ME as a combination of the Born differential sections with the redefined scattering angle θ .

¹¹ Other similar choices of the angle in the Born distribution are also perfectly valid within the LO MC.

above we only need directions of the vectors \vec{p}_{0F} and \vec{p}_{0B} , which are the same as of the hadron beams. The variable $\hat{s} = sx_Fx_B = (q_1 + q_2)^2$ is the effective mass squared of the heavy vector boson. Finally, we specify the lightcone variables α_j and β_j of the emitted gluon for j in the F and B parts of the phase space

$$\begin{aligned}\alpha_j &= 1 - z_{Fj}, & \beta_j &= \alpha_j e^{2(\eta_j - \Xi)}, & \text{for } j \in F, \\ \beta_j &= 1 - z_{Bj}, & \alpha_j &= \beta_j e^{-2(\eta_j - \Xi)}, & \text{for } j \in B.\end{aligned}$$

The above relations are explained in Ref. [4] as resulting directly from the kinematical projection operators extracting the LO part from the exact matrix element. Note that variables α_j and β_j in the above relations are defined in terms of \bar{k}_j^μ , which do not obey the overall 4-momentum conservation. The transformation $\bar{k}_j^\mu \rightarrow k_j^\mu$ and its inverse (where k_j^μ do obey 4-momentum conservation) are defined explicitly in the above work. Slightly improved (LO level) kinematical mapping, better suited for the NLO-corrected hard process will be proposed at the end of Section 4.

The exact phase space integration of Eq. (3) including W_{MC}^{NLO} of Eq. (5) is again possible, see Ref. [4] for details, providing a compact expression for the total cross section

$$\begin{aligned}\sigma_1 &= \int_0^1 dx_F dx_B dz D_F(t, x_F) D_B(t, x_B) \sigma_B(szx_Fx_B) \\ &\quad \times \{\delta_{z=1}(1 + \Delta_{S+V}) + C_{2r}(z)\},\end{aligned}\tag{7}$$

where $C_{2r}(z) = \frac{2C_F\alpha_s}{\pi} \left[-\frac{1}{2}(1-z)\right]$ was derived in Ref. [4].

3. Numerical results

In the following, we shall first check that the simple formula of Eq. (4) with two collinear PDFs agrees numerically with the parton shower MC of Eq. (3) with the LO hard process ($W_{MC}^{NLO} = 1$). Once the above “LO benchmark calibration” is successful, we shall check numerically whether the NLO formula of Eq. (7) agrees with the MC integration of Eq. (3), switching on the NLO correcting weight W_{MC}^{NLO} of Eq. (5). In both MC exercises we expect deviations only up to statistical MC error, or other imperfections of the numerical implementations.

3.1. LO benchmark

Figure 1 represents a “calibration benchmark” for the overall normalization at the LO level. In fact, we show in Fig. 1 the properly normalized distribution of the variable $\eta_W^* = \frac{1}{2} \ln(x_F/x_B)$. In the collinear limit, this variable represents the rapidity of W boson. This variable will differ substantially from the true rapidity of the W boson in the presence of the gluon with hard transverse momentum, but this is an acceptable approximation in the current LO exercise. The W mass distribution with the sharp Breit–Wigner resonance lineshape is not very interesting and we do not show it here.

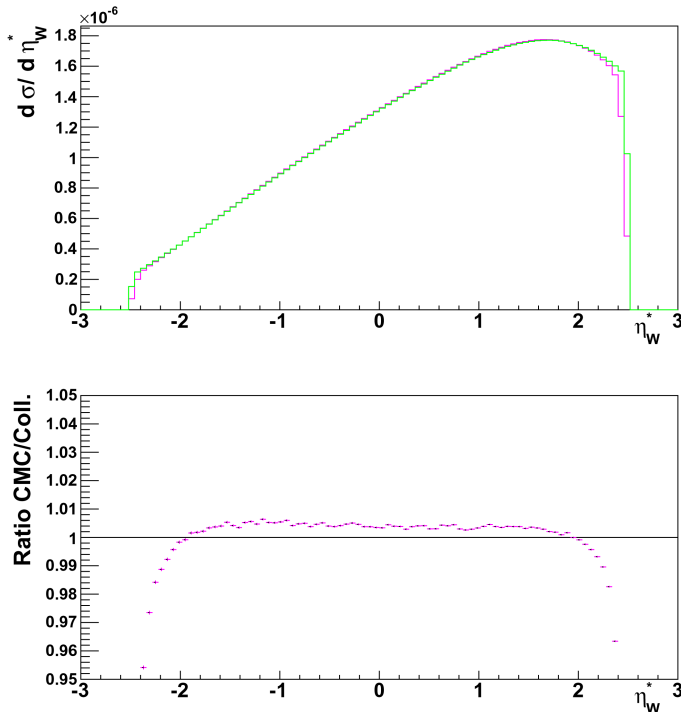


Fig. 1. In the upper plot, the LO distribution of $\eta_W^* = \frac{1}{2} \ln(x_F/x_B)$ from the CMC LO parton shower (black/purple) and from the strictly collinear formula (grey/green) are shown. The lower plot shows the ratio of the two, the agreement of $< 0.5\%$ is obtained.

In Fig. 1, one of the distributions is from the MC generation of the variables (x_F, x_B) according to 2-dimensional integrand of Eq. (4). This is done using the general purpose MC program FOAM [16]. However, in this MC we need the collinear PDF $D(t, x)$ in the entire range of x and t as an input. This distribution has been obtained from a separate high statistics run (10^{10} events) of a simple Markovian MC (MMC), recording the resulting

$D(t, x)$ in the 2-dimensional table (a finite grid). In fact, this MMC run solves the LO DGLAP equation (for gluonstrahlung LO kernel) using the MC method, similarly as in Refs. [17, 18]¹². From the look-up table recorded during the MMC run, a simple interpolation is employed to obtain $D(t, x)$ for any values of t and x in the next step, that is, in the 2-dimensional integrand used by FOAM.

Another distribution in Fig. 1 comes from the full scale MC generation (four-momenta conserving) according to Eq. (3). The MC run with 10^8 events was used. In the MC implementation we cannot use the Markovian method because of the narrow Breit–Wigner peak due to a heavy boson propagator. We could employ a backward evolution algorithm of Ref. [20], but instead we have opted to employ a variant of the constrained MC (CMC) technique of Ref. [13]. In fact, we combine two CMC modules and FOAM into one MC generating gluon emission from the incoming quark and antiquark which annihilate into the W boson. The LO hard process ME of the W boson production is implemented¹³, FOAM is taking care of the generation of the variables x_F, x_B, x_{F0}, x_{B0} and the sharp Breit–Wigner peak in $\hat{s} = sx_F x_B$, then initial parameters for two CMC modules are set and the gluon four-momenta \bar{k}_j^μ are generated. Once they are mapped into k_j^μ , following the prescription defined in Ref. [4], the overall energy-momentum conservation is achieved.

Figure 1 demonstrates a very good numerical agreement between $d\sigma/d\eta_W^*$ from our full scale LO parton shower MC of Eq. (3) and the simple formula of Eq. (4) in the strict collinear kinematics (just convolution of two PDFs and the Born cross section). The LO MC is working in the standard phase space, with the exact 4-momentum conservation and agrees with precision $< 0.5\%$ with the simple collinear formula of Eq. (4). The visible numerical bias is most likely due to finite size of the grid used to parametrize PDFs from the MMC run.

3.2. Numerical test of NLO correction

Having cross-checked very precisely the overall normalization of our LO MC, we are now ready to do a similar cross-check in the case of the NLO-corrected hard process.

¹² The use of the MC method is not mandatory here — we could solve it using finite step methods, as in Ref. [19].

¹³ In the presented MC exercise, the average over angular distribution of the W boson decay products is taken. This is irrelevant for the conclusions of our study and this averaging can be undone rather easily.

Figure 2 represents a principal (technical) test and *proof of concept* of our new methodology for implementing the NLO corrections to the hard process in the parton shower MC. The NLO correction to the η_W^* distribution is obtained, on the one hand, within the full scale parton shower MC featuring the NLO-corrected hard process as in Eqs. (3) and (5), and, on the other hand, with a simple collinear formula of Eq. (7) in which two PDFs are convoluted with the analytical function $C_{2r}(z)$, the “coefficient function” for the hard process. In Fig. 2, we present the NLO corrections obtained using both calculations. The LO component, cross-checked in the previous section, is present in the MC but not shown in this plot in order to increase the “resolution”. In Fig. 2, we also include the ratio of the NLO corrections from the two sources.

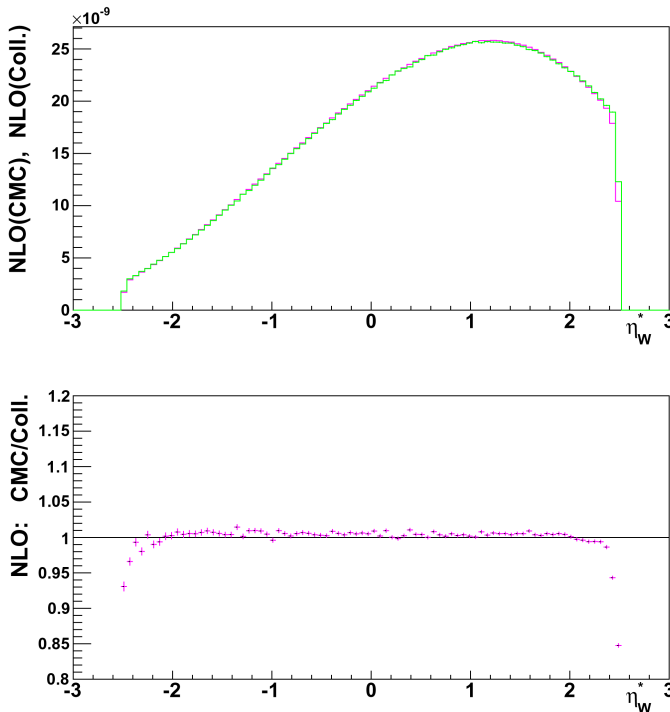


Fig. 2. The pure (—) NLO correction to the distribution of $\eta_W^* = \frac{1}{2} \ln(x_F/x_B)$ in CMC LO parton shower in W boson production (black/purple). It agrees with the strictly collinear formula (grey/green) to within $< 1\%$ of the NLO correction itself.

As seen in Fig. 2, the result of the parton shower MC with the NLO-corrected hard process and the result of the simple collinear formula of Eq. (7) agree very well, within the statistical error.

In Fig. 2, we see only the NLO corrections, but how big is the NLO correction with respect to the LO? We show this in Fig. 3, where both the LO and NLO components are compared, and the NLO/LO ratio is plotted as well. As we see, the NLO correction to the rapidity-like variable for the W boson is only about 1.5% of LO, and this is unusually small.

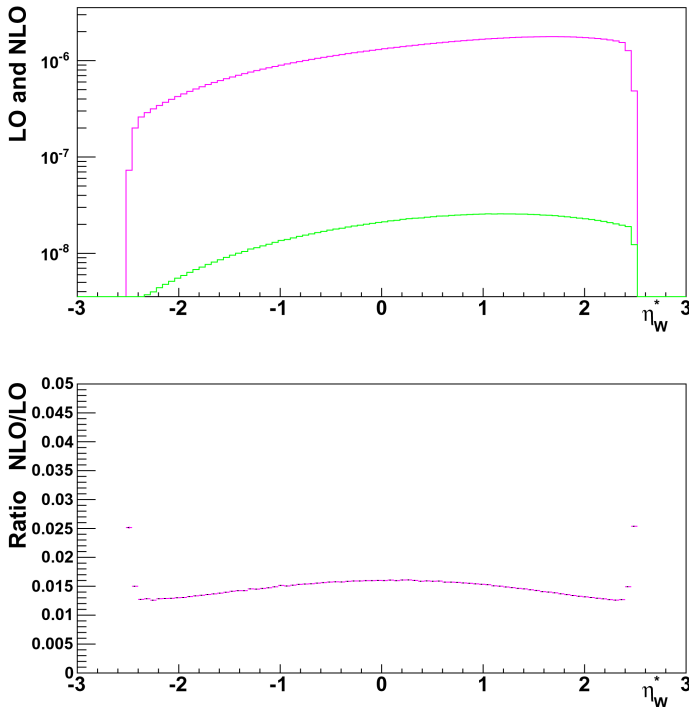


Fig. 3. The comparison of the LO (black/purple) and of the pure (–) NLO corrections (grey/green) to the distribution of $\eta_W^* = \frac{1}{2} \ln(x_F/x_B)$; the overall normalization is in GeV^{-2} .

For this particular hard process the NLO correction is negative, hence in both Figs. 2 and 3 it is multiplied by the factor (-1) , in order to facilitate visualization of the results.

At the technical level, the inclusion of the NLO correction in the parton shower MC is straightforward, we are just activating $W_{\text{MC}}^{\text{NLO}}$ of Eq. (5). In fact, MC is providing the LO and NLO-corrected results in a single MC run with weighted events. The $W_{\text{MC}}^{\text{NLO}}$ weight is well behaved, strongly peaked near $W_{\text{MC}}^{\text{NLO}} = 1$, positive, and without long-range tails. The distribution of this weight is shown in Fig. 4. In the MC implementing the collinear formula of Eq. (7), we again use FOAM, but now the generation space is 3-dimensional due to the presence of additional variable z .

Note that in all numerical results shown so far we have put $\Delta_{V+S} = 0$, as it is completely unimportant for the purpose of the presented numerical analysis. For our study, we also used toy initial distributions $d_0(q_0, t)$, which were parametrized as follows

$$\begin{aligned} xD_{q \in p}(x, 1 \text{ GeV}) &= 2xu(x) + xd(x) + \frac{1}{2}xs(x), \\ 2xu(x) &= 2.19 x^{1/2}(1-x)^3, \\ xd(x) &= 1.23 x^{1/2}(1-x)^4, \\ xs(x) &= 1.35 x^{0.2}(1-x)^7. \end{aligned}$$

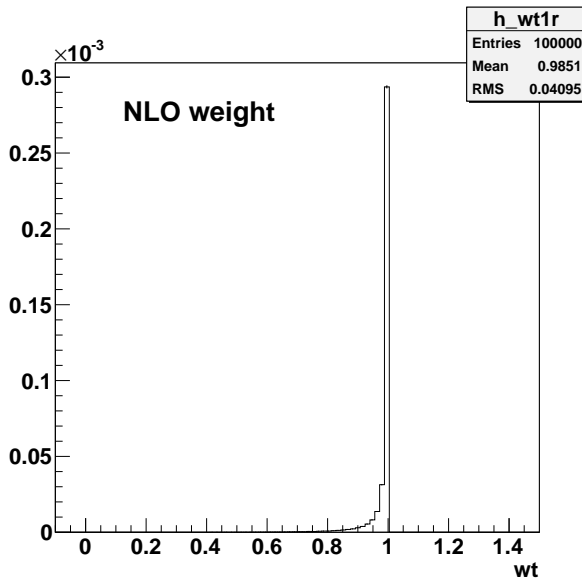


Fig. 4. The distribution of the NLO weight W_{MC}^{NLO} of Eq. (5).

4. Discussion and comparison with other methods

The new method of introducing the NLO corrections in the hard process proposed in Ref. [4] and tested in this work is clearly very different from the well established MC@NLO [21] and POWHEG [22, 23] methodologies. Ref. [4] offers a limited discussion on these differences. Having at hand MC numerical implementation, we may elaborate on certain issues in more detail, in particular, we are going to show numerical results illustrating differences with the POWHEG technique.

At first sight, the most striking difference with the POWHEG and MC@NLO techniques are:

- “Democratic” summation over all emitted gluons, without deciding explicitly which gluon is the one involved in the NLO correction and which ones are merely “LO spectators” in the parton shower.
- The absence of $(1/(1-z))_+$ distributions in the real part of the NLO corrections (kinematics independence of the virtual + soft correction).

In the following, we shall elaborate mainly on the first point, analysing in a detail how $W_{\text{MC}}^{\text{NLO}}$ of Eq. (5) is distributed over the multigluon phase space. In order to make the discussion maximally transparent, let us consider a simplified weight

$$W_{\text{MC}}^{\text{NLO}} = 1 + \sum_{j \in \text{F}} W_j^{\text{NLO}}, \quad W_j^{\text{NLO}} = \frac{\tilde{\beta}_1(q_1, q_2, \bar{k}_j)}{\bar{P}(z_{\text{F}j}) d\sigma_{\text{B}}(\hat{s}, \hat{\theta})/d\Omega} \quad (8)$$

which is limited to one ladder (one hemisphere). Moreover, we put it on top of the MC modelling gluon emissions from single quark¹⁴, essentially the multigluon distribution of Eq. (1).

We start by examining the inclusive distribution of gluons on the Sudakov logarithmic plane of rapidity ξ and variable $v = \ln(1-z)$. This is shown in Fig. 5 (a). The distribution looks as expected, and the flat plateau represents IR singularity $2C_{\text{F}} \frac{\alpha_{\text{s}}}{\pi} d\xi \frac{dz}{1-z}$ (for constant α_{s}) with the drop by factor $1/2$ towards $z = 0$, due to $\frac{1+z^2}{2}$ factor in the LO kernel.

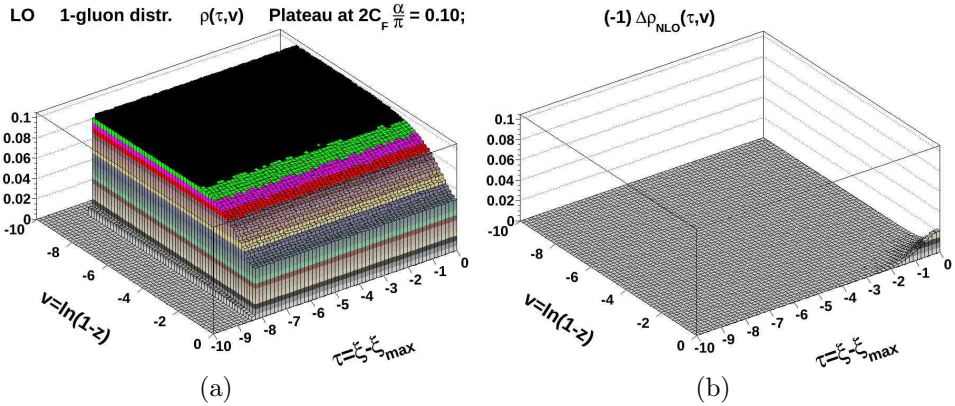


Fig. 5. (a) The inclusive distribution of gluons on the log Sudakov plane of rapidity $t = \xi_{\text{max}}$ and $v = \ln(1-z)$. (b) Contributions from all gluons weighted with the component weight W_j^{NLO} .

¹⁴ We use the Markovian MC implementation, but optional use of the CMC would provide identical results. We use quite a wide range of t , corresponding to $\sqrt{s} = 7 \text{ TeV}$.

In Fig. 5(b), we show contributions from all gluons weighted with the component weight $-W_j^{\text{NLO}}$ of Eq. (8). (We insert a minus sign in order to facilitate visualization.) Here we see that the NLO contribution is concentrated in the area near the rapidity of the hard process $t = \xi_{\text{max}}$, which has to be true for the genuine NLO contribution. On the other hand, the fact that the NLO correction dies out towards the IR limit $z \rightarrow 1$ is not guaranteed in the collinear factorization. It results from the conscious choice that our LO differential distributions reproduce the correct IR limit not only in LO but also in NLO and in the entire phase space¹⁵.

Another important point is the completeness of the phase space near the $(z = 0, t = \xi_{\text{max}})$ phase space corner. Both POWHEG and MC@NLO use standard LO MCs which feature an empty “dead zone” in this region¹⁶, which is critical for the completeness of the NLO corrections in the hard process. They have to fill in this empty part of the phase space with MC events according to the correct LO+NLO distribution. Correcting for this deficiency of the standard LO MC requires non-trivial effort. In our case, the problem of the phase space incompleteness is absent¹⁷ and we simply re-weight the LO distribution (MC events) to the NLO level.

Finally, we also see that the NLO correction is very small, which might be a general feature of the new method. It is mainly due to the absence of the $(1/(1-z))_+$ terms in the NLO correction — this is a separate issue discussed in Ref. [4], see also a few remarks below.

Looking at Fig. 5 it is tempting to conclude that the dominant contribution to $\sum_j W_j^{\text{NLO}}$ may come from the gluon with the highest $\ln k_j^T \sim \xi_j + \ln(1-z_j)$, that is the closest to the hard process corner $(z = 0, t = \xi_{\text{max}})$. We may easily relabel gluons generated in the MC, $\sum_j \rightarrow \sum_K$, such that they are ordered in the variable $\kappa_K = \xi_K + \ln(1-z_K)$, with $K = 1$ being the hardest one ($\kappa_{K+1} < \kappa_K$).

In Fig. 6, we show a split of the inclusive distribution of Fig. 5(a) into the $K = 1$ component (hardest gluon in k^T) and the rest $K > 1$. As we see, the $K = 1$ component saturates/reproduces the original complete distribution of Fig. 5(a) over all the region, where the NLO correction (Fig. 5(b)) is non-negligible. This is exactly the observation on which POWHEG technique is built! Moreover, as noticed by the POWHEG authors, taking the $K = 1$ component is sufficient to reproduce the complete NLO correction (up to NNLO).

¹⁵ Older version of the standard LO MCs do not always reproduce the correct soft gluon limit beyond the LO level.

¹⁶ This is due to the use of the boost transformation in the standard LO MCs to get the overall four-momentum conservation. We avoid this transformation (problem) as we use the rescaling transformation only in $\bar{k}_j \rightarrow k_j$ in the LO MC.

¹⁷ Of course, reconstructing the LO parton shower also requires non-trivial effort.

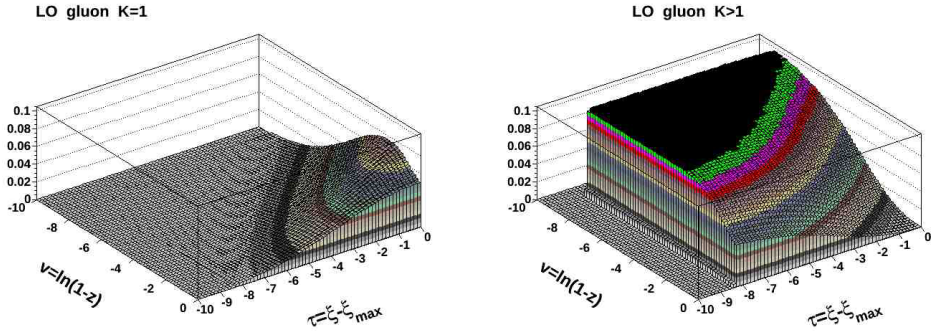


Fig. 6. The inclusive distribution of gluons of Fig. 5(a) split into the hardest (in k^T) gluon (left) and the rest (right).

Let us check numerically the above statements by means of comparing the NLO correction to the $x = x_0 \prod_j z_j$ distribution from $\sum_j W_j^{\text{NLO}}$ and from $W_{K=1}^{\text{NLO}}$. This comparison is shown in Fig. 7. As we see, the $K = 1$ component saturates the entire sum very well, whereas the $K = 2$ component is quite small. A natural question is: why bother to keep the entire sum instead of taking only the $K = 1$ contribution? In fact we can, which is a valuable feature of our scheme. However, we stress that in the POWHEG scheme the $K = 1$ gluon is generated in the MC separately in the first step and other gluons are generated (by the LO parton shower MC) in the next step. This is fine and easy if the LO MC uses k^T -ordering, while in the case of the LO MC with angular/rapidity-ordering additional effort of generating the so-called vetoed showers and truncated showers is needed in the POWHEG method. In our method, the angular ordering is used but the vetoed/truncated showers are not needed, even if we replace the sum

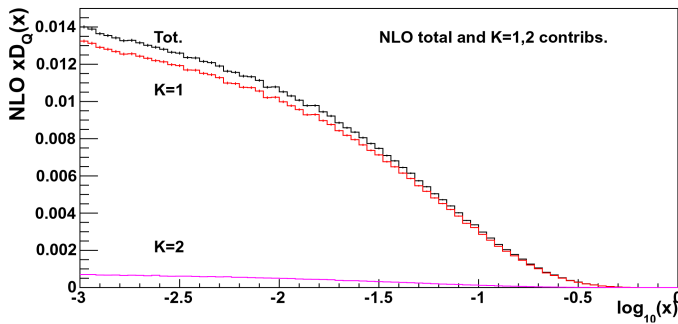


Fig. 7. The full NLO correction $\sum_j W_j^{\text{NLO}}$ and its two hardest (in k^T) components $W_{K=1}^{\text{NLO}}$, $W_{K=2}^{\text{NLO}}$ as a function of $x = \prod_j z_j$.

$\sum_j W_j^{\text{NLO}}$ by $K = 1$ component $W_{K=1}^{\text{NLO}}$. Is there any rationale for keeping the sum over gluons in NLO weight at all? There are two reasons for keeping it, at least optionally: (a) the valuable cross-check of the NLO MC against the simple collinear formula of Eq. (7) is exact only if we keep the sum, (b) it may turn out that keeping the sum reduces missing NNLO corrections. In our opinion one should keep both versions and check which one fits better the complete NNLO or better agrees with additional resummations beyond LO.

As an additional illustration for the above discussion, in Fig. 8, we show the distribution of gluons ordered in rapidity, starting from the gluon with the maximum rapidity, the closest to hard process. As we see, the gluon distribution with the highest rapidity $\xi \sim \xi_{\text{max}}$ ($J = 1$) features a ridge extending towards the soft region. It is important to notice that the width of this ridge goes to zero when $\epsilon \rightarrow 0$ in the IR cut-off $(1-z) < \epsilon$. Hence, sooner or later the gluon with the highest ξ will not be able to reproduce/saturate the gluon distribution in the NLO corner close to hard process, and the NLO correction will be highly incomplete. In the k^T -ordering this is not the case, of course.

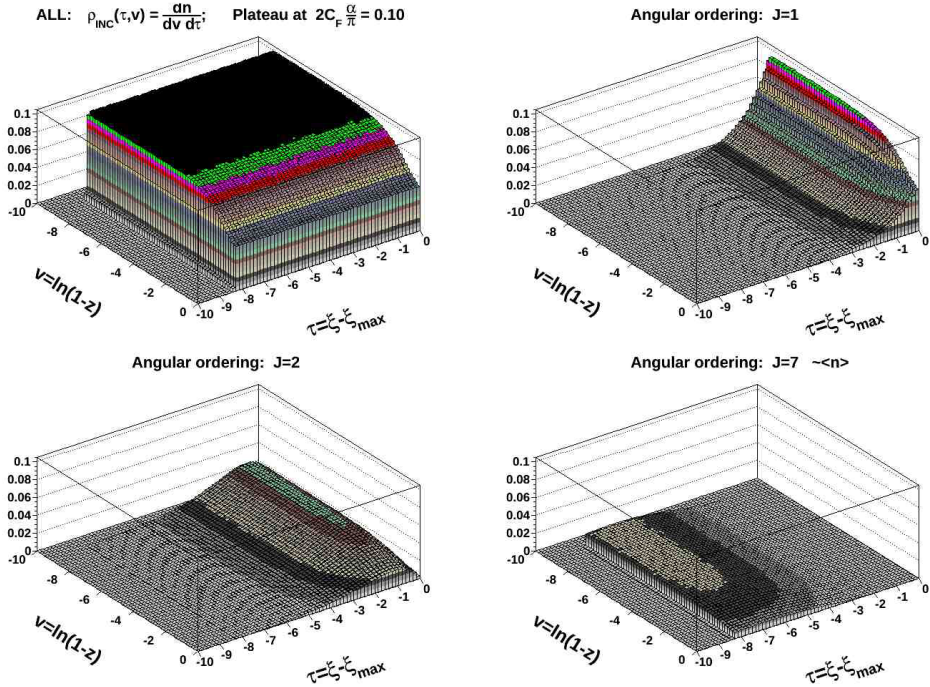


Fig. 8. The distribution of gluons ordered in rapidity, as in our basic LO MC.

In the above, we have mainly discussed the differences of our MC with the POWHEG method in which, similarly to our case, the negative MC weight is not allowed. The MC@NLO method roughly corresponds to generating in a separate MC branch events according to non-positive NLO correcting distribution. In the same MC branch, events filling the empty phase space near the hard process corner are also added¹⁸.

Both MC@NLO and POWHEG feature the $(1/(1-z))_+$ components in the NLO corrections, which are the source of the practical complications there, while they are absent in our approach. In MC@NLO and POWHEG case these $(1/(1-z))_+$ corrections act effectively as the “in-flight” translation of the PDFs from the $\overline{\text{MS}}$ collinear factorization scheme (FS) to the FS used effectively in the MC, (see Ref. [4]). We propose to shift this translation beyond the MC, as a rather simple redefinition of PDFs which should be done “off line”, from the point of view of MC. The above issue requires a dedicated study (in preparation), and is also closely related to the upgrade of the ladder part of the MC to the NLO level.

Having in mind that the considered method is more general, and can be also applied for introducing the NLO corrections in the middle of the ladder [24, 25], it is an interesting question whether limiting the sum $\sum_j W_j^{\text{NLO}}$ to one (or two) terms would/could be used in order to upgrade the QCD evolution in the parton shower to the complete NLO level, which would open many new promising avenues in the development of the high quality QCD parton shower MCs for LHC and other colliders. This question will be addressed in the forthcoming study in Ref. [26].

The present work provides a numerical cross-check of the ideas outlined in Ref. [4]. We briefly mention the most urgent future studies which will necessarily follow this work (some are already completed but unpublished). The two most important issues are: (i) adjusting the choice of Ξ at NLO level, and (ii) selecting a better choice/definition of initial PDF. Also, adding missing graphs for the NLO corrections, that is graphs with gluon to quark transitions is needed. This should be simpler than the presented gluon-strahlung contributions due to lack of IR singularities.

The present choice of the rapidity boundary $\Xi = 0$ is good at the LO level, and it also correctly reproduces the integrated NLO cross section. However, at the exclusive level, the exact NLO distributions must be properly reproduced in the limit when all gluons but one are collinear (have small k^T), for instance, the rapidity difference between the heavy boson and the hardest (in k^T) gluon. For the above aim the best choice is to identify Ξ with the rest system of the heavy boson and the hardest gluon η^* . This can be easily obtained by means of refining the mapping $\bar{k}_i \rightarrow k_i$ in such a way

¹⁸ This, luckily, reduces the number of events with the negative weight.

that it is used twice. For the first time with $\Xi = 0$, then the rapidity η^* is determined and $\bar{k}_i \rightarrow k_i$ mapping is repeated with $\Xi = \eta^*$. Obviously, some gluons will be reclassified as belonging to another initial beam ladder¹⁹. The above solution was already tested and works correctly.

Concerning further refinements on the initial PDF, this issue would be resolved automatically if MC was fitted to the experimental data or if the PDFs have been fitted within the MC scheme. If the initial PDF is to be taken from a standard library of PDFs in the $\overline{\text{MS}}$ scheme, then it will be necessary to correct it using the difference of the counterterms of the $\overline{\text{MS}}$ and MC schemes (see Eq. (44) in [4]). From the classic analysis [27] of NLO corrections to the DY process, it is known that this correction will be large and dominated by the term $\sim \left(\frac{\ln((1-z)^2/z)}{1-z} \right)_+$, in the region where quark distribution²⁰ is strongly varying in x . Note that in POWHEG method the above correction is implemented in the MC by means of explicit generation of the variables in the convolution implementing NLO corrections and the corresponding manipulation on four-momenta is done. In contrast, in our method NLO corrections are included entirely through MC weight and no extra kinematics transformations are needed (beyond these of the LO MC modelling).

In the above context, interesting numerical results are presented in Ref. [28] — they illustrate the size and location of the x -variation in PDFs due to kinematics manipulations in POWHEG driven by NLO corrections. In our method, the entire kinematical modification of the longitudinal parton fraction x is due to the LO mapping and the shape modification due to the NLO weight. We expect this effect to be less sizable in our method, but a separate study would be needed to verify it.

5. Summary and outlook

A new methodology of adding the QCD NLO corrections to the hard process in the initial state Monte Carlo parton shower is tested numerically using heavy boson production at hadron–hadron colliders. The ladder parts of the parton shower are modelled in the LO approximation, also using these new methods. The presented numerical results prove that the basic concept of the new methodology works correctly in the numerical environment of a Monte Carlo parton shower. The differences with the well established methods of MC@NLO and POWHEG are briefly discussed. Also, possible refinements of the method are indicated.

¹⁹ Luckily, this “flow” of gluons from one to another hemisphere does not influence the overall MC weight.

²⁰ Similar phenomenon will occur for the gluon distribution.

Clearly the "proof of concept" is successful, and more work is required before a practical application will emerge.

This work is partly supported by the Polish Ministry of Science and Higher Education grant No. 1289/B/H03/2009/37, the Polish National Science Centre grant DEC-2011/03/B/ST2/02632, the NCBiR grant LIDER/02/35/L-2/10/NCBiR/2011, the Research Executive Agency (REA) of the European Union Grant PITN-GA-2010-264564 (LHCPhenoNet), the U.S. Department of Energy under grant DE-FG02-04ER41299 and the Lightner-Sams Foundation. One of the authors (S.J.) is grateful for the partial support and warm hospitality of the TH Unit of the CERN PH Division, while completing this work.

REFERENCES

- [1] D.J. Gross, F. Wilczek, *Phys. Rev. Lett.* **30**, 1343 (1973); H.D. Politzer, *Phys. Rev. Lett.* **30**, 1346 (1973); D.J. Gross, F. Wilczek, *Phys. Rev.* **D8**, 3633 (1973); H.D. Politzer, *Phys. Rep.* **14**, 129 (1974).
- [2] D.J. Gross, F. Wilczek, *Phys. Rev.* **D9**, 980 (1974).
- [3] H. Georgi, H.D. Politzer, *Phys. Rev.* **D9**, 416 (1974).
- [4] S. Jadach *et al.*, arXiv:1103.5015v2 [hep-ph].
- [5] B. Ermolaev, V.S. Fadin, *JETP Lett.* **33**, 269 (1981).
- [6] Y. Dokshitzer, V. Khoze, A. Mueller, S. Troyan, *Basics of Perturbative QCD*, Editions Frontieres, 1991.
- [7] M. Slawinska, A. Kusina, *Acta Phys. Pol. B* **40**, 2097 (2009) [arXiv:0905.1403v1 [hep-ph]].
- [8] M. Ciafaloni, *Nucl. Phys.* **B296**, 49 (1988); S. Catani, F. Fiorani, G. Marchesini, *Phys. Lett.* **B234**, 339 (1990); *Nucl. Phys.* **B336**, 18 (1990).
- [9] G. Marchesini, *Nucl. Phys.* **B445**, 49 (1995) [arXiv:hep-ph/9412327v1].
- [10] S. Catani, B.R. Webber, G. Marchesini, *Nucl. Phys.* **B349**, 635 (1991).
- [11] G. Marchesini, B.R. Webber, *Nucl. Phys.* **B310**, 461 (1988).
- [12] H. Jung *et al.*, *Eur. Phys. J.* **C70**, 1237 (2010) [arXiv:1008.0152v1 [hep-ph]].
- [13] S. Jadach *et al.*, *Comput. Phys. Commun.* **180**, 675 (2009) [arXiv:hep-ph/0703281v2].
- [14] F.A. Berends, R. Kleiss, *Nucl. Phys.* **B178**, 141 (1981).
- [15] S. Alioli, K. Hamilton, E. Re, *J. High Energy Phys.* **1109**, 104 (2011) [arXiv:1108.0909v2 [hep-ph]].
- [16] S. Jadach, *Comput. Phys. Commun.* **152**, 55 (2003) [arXiv:physics/0203033v2].

- [17] S. Jadach, W. Placzek, M. Skrzypek, P. Stoklosa, *Comput. Phys. Commun.* **181**, 393 (2010) [arXiv:0812.3299v2].
- [18] K. Golec-Biernat, S. Jadach, W. Placzek, M. Skrzypek, *Acta Phys. Pol. B* **37**, 1785 (2006) [arXiv:hep-ph/0603031v1].
- [19] M. Botje, *Comput. Phys. Commun.* **182**, 490 (2011) [arXiv:1005.1481v3].
- [20] T. Sjostrand, *Phys. Lett.* **B157**, 321 (1985).
- [21] S. Frixione, B.R. Webber, *J. High Energy Phys.* **0206**, 029 (2002) [arXiv:hep-ph/0204244v2].
- [22] P. Nason, *J. High Energy Phys.* **0411**, 040 (2004) [arXiv:hep-ph/0409146v1].
- [23] S. Frixione, P. Nason, C. Oleari, *J. High Energy Phys.* **0711**, 070 (2007) [arXiv:0709.2092v1 [hep-ph]].
- [24] S. Jadach, M. Skrzypek, A. Kusina, M. Slawinska, *PoS RADCOR2009*, 069 (2010) [arXiv:1002.0010v1 [hep-ph]].
- [25] M. Skrzypek *et al.*, *Acta Phys. Pol. B* **42**, 2433 (2011) [arXiv:1111.5368v1 [hep-ph]].
- [26] S. Jadach, A. Kusina, M. Skrzypek, Report IFJPAN-IV-2012-7, in preparation.
- [27] G. Altarelli, R.K. Ellis, G. Martinelli, *Nucl. Phys.* **B157**, 461 (1979).
- [28] F. Hautmann, H. Jung, arXiv:1209.6549v1 [hep-ph].